Ultimate Internal Pressure Capacity of Concrete Containment Structures

C.N. Krishnaswamy, R. Namperumal, A. Al-Dabbagh
Sargent and Lundy Engineers, 55 East Monroe Street, Chicago, Illinois 60603, U.S.A.

SUMMARY

Lesson learned from the accident at Three-Mile Island nuclear plant has necessitated the computation of the ultimate internal pressure capacity of containment structures as a licensing requirement in the U.S. In general, a containment structure is designed to be essentically elastic under design accident pressure. However, as the containment pressure builds up beyond the design value due to a more severe postulated accident, the containment response turns nonlinear as it sequentially passes through cracking of concrete, yielding of liner plate, yielding of rebar, and yielding of post-tensioning tendon (if the containment concrete is prestressed). This paper reports on the determination of the ultimate internal pressure capacity and nonlinear behavior of typical reinforced and prestressed concrete BWR containments.

The probable modes of failure, the criteria for ultimate pressure capacity, and the most critical sections are described. Simple equations to hand-calculate the ultimate pressure capacity and the nonlinear behavior at membrane sections of the containment shell are presented.

A nonlinear finite element analysis performed to determine the nonlinear behavior of the entire shell including nonmembrane sections is briefly described. The analysis model consisted of laminated axisymmetric shell finite elements with nonlinear stress-strain properties for each material.

Results presented for typical BWR concrete containments include nonlinear response plots of internal pressure versus containment deflection and strains in the liner, rebar, and post-tensioning tendons at the most stressed section in the shell. Leak-tightness of the containment liner and the effect of thermal loads on the ultimate capacity are discussed.

1. INTRODUCTION

This paper reports on the determination of the ultimate internal pressure capacity of a reinforced concrete BWR Mark III Containment shown in Figure 1 and a prestressed concrete BWR Mark II Containment shown in Figure 2. The design accident internal pressure for these containments is 15 psig and 45 psig, respectively. The principal dimensions of the containments are shown in the figures.

Both containments are lined on the inside with a 1/4 inch thick steel plate to ensure leak-tightness. The containments are each provided with an equipment hatch, personnel air locks, and other necessary electrical and piping penetrations through the wall.

The probable modes of failure and the critical containment sections are described in Section 2. Conservative criteria for determining structural failure and ultimate capacity are defined in Section 3. Equilibrium equations to help hand-compute the ultimate capacity and nonlinear response at membrane sections of the concrete shell are presented in Section 4. A nonlinear axisymmetric finite element analysis performed to obtain the response of the entire shell including nonmembrane sections and to verify the hand-computed results is described in Section 5. Results of the analysis, leak-tightness of liner, and thermal effects are discussed in Section 6.

Although the paper relates to BWR concrete containments, the mechanics and observations reported here are also applicable to PWR concrete containments.

2. POSSIBLE FAILURE MODES AND CRITICAL SECTIONS

As the internal pressure builds up beyond the design value due to a more severe postulated accident, failure of the containment pressure boundary can result from one or more of the following causes:

a. Rupture of reinforcing steel, if the containment is of reinforced concrete.
b. Failure of concrete in secondary compression.
c. Failure in flexural shear at discontinuities.
d. Failure in peripheral shear around penetrations.
e. Failure of steel pressure retaining components by buckling or by rupture.
f. Rupture of post-tensioning tendons, if the containment is of prestressed concrete.
g. Separation of the steel drywell head (BWR Mark II) from the containment wall.

The potential critical sections associated with the failure modes of the pressure boundary backed by concrete are shown in Figures 1 and 2.

3. FAILURE CRITERIA FOR ULTIMATE CAPACITY

Though the ultimate failure of the containment may occur well past general yielding of the critical section with attendant large displacements, the capacity of the containment is defined here as the attainment of any one of the following limits:

a. Tensile yielding of reinforcing steel resulting in a state of general yielding of any section, if the containment is of reinforced concrete.
b. Tensile yielding of post-tensioning tendons (corresponding to a strain of .01 in/in) resulting in a state of general yielding of any section, if the containment is of prestressed concrete.

c. Shear capacity of the containment in flexural shear or peripheral shear.

d. Buckling or yielding of steel pressure retaining components.

These limits are conservative and therefore there is some reserve capacity beyond the limits defined above.

Failure by criterion (d) is not included in the analysis described in Sections 4 and 5.

4. EQUATIONS OF EQUILIBRIUM

In general, the containment structure is designed to be essentially elastic under design pressure. However, as the postulated internal overpressure builds up and reaches the ultimate, the containment response will turn nonlinear as it sequentially passes through cracking of concrete, yielding of liner plate, yielding of reinforcing steel, and yielding of tendons (if the containment is of prestressed concrete). For these critical response stages, the internal pressure capacity at a membrane section can be predicted by means of the following equations based on equilibrium considerations.

The internal force P per foot width of the shell at a membrane section can be computed as:

Force/ft at the start of pressurization, P_o = Dead Load + Prestress (1)

Force/ft at concrete cracking, $P_{cr} = A_c E_c \epsilon_{cr} + (n-1)\ (A_l + A_s + A_t)\ E_c \epsilon_{cr} + P_o$ (2)

Force/ft just after concrete cracking = $P_{cr} = E_s \epsilon'_{cr}\ (A_l + A_s + A_t) + P_o$ (3)

Force/ft at liner yielding, $P_{yl} = E_s\ (\epsilon_{yl} - \epsilon'_{cr})\ (A_l + A_s + A_t) + P_{cr}$ (4)

Force/ft at rebar yielding, $P_{ys} = E_s\ (\epsilon_{ys} - \epsilon_{yl})(A_s + A_t) + P_{yl}$ (5)

Force/ft at tendon yielding, $P_{yt} = E_s\ (\epsilon_{yt} - \epsilon_{ys})\ A_t + P_{ys}$ (6)

where,

A_c	= Gross area of concrete per foot of shell
A_l, A_s, A_t	= Area of liner, rebar, and tendon, respectively per foot of shell
ϵ_{cr}	= Cracking strain in concrete
ϵ'_{cr}	= Strain just after concrete cracking
$\epsilon_{yl}, \epsilon_{ys}, \epsilon_{yt}$	= Yield strain in liner, rebar, and tendon, respectively
E_c	= Modulus of elasticity for concrete
E_s	= Modulus of elasticity for steel (liner, rebar, and tendon)
n	= Modular ratio

The internal pressure corresponding to any of the response stages is then obtained as

$p = P/R$ (7)

where P = Force per foot of shell

R = Radius of the containment at the section considered

Also, the radial displacement, $\Delta = R.\epsilon$ (8)

Equations (2) through (6) include the liner as a strength element. If the liner acts as a non-strength element, A_l should be set equal to zero in these equations.

Using the above equations and the properties listed in Figures 1 and 2, the response and pressure capacity of the example containments were computed at the most stressed section under design pressure which is the membrane section near midheight of the containment cylinder.

5. FINITE ELEMENT ANALYSIS

A nonlinear axisymmetric finite element analysis of these containment shells under incremental internal pressure was performed to verify the hand-computed results and to determine the nonlinear behavior of the entire shell including nonmembrane sections. The analysis model consisted of laminated shell finite elements to represent the liner, concrete, and reinforcing steel layers. Nonlinear stress-strain property of each material was considered. Only material nonlinearity was considered; geometric nonlinearity was ignored because of small displacements for concrete shell structures.

Concrete was idealized as a linearly elastic and perfectly plastic material in compression and linearly elastic up to $6\sqrt{f'_c}$ in tension. Failure criterion under biaxial stresses is shown in Figure 3.

For the prestressed concrete containment, post-tensioning tendons were modeled as laminated shell elements. The independent longitudinal displacement of their unbonded length between the anchor points was also simulated. A trilinear stress-strain relationship shown in Figure 4 was used for the tendons. Each tendon was modeled as a pair (twin) of tendons with two separate perfectly elastic-plastic stress-strain curves which, when combined, simulated the trilinear stress-strain relationship of the tendon. This approach is graphically shown in Figure 4.

Material strengths obtained from uniaxial test specimens were used. The dead load of the structure, the hydrostatic load on the suppression pool boundary, post-tension loads, and the incremental internal pressure were applied simultaneously. Incremental internal pressure was applied as the structure passed through the critical response stages of concrete cracking, liner yielding, rebar yielding, and tendon yielding.

The computer program, DYNAX, used for the shell analysis is based on a report by Ghosh and Wilson [1]. The mechanics of nonlinear analysis of laminated shells is described in detail by Khatua, Radwan, and Sarne [2] and by Lin and Scordelis [3]. The internal pressure due to the postulated accident was treated as quasi-static based on the investigation by Kamil, et. al [4].

6. DISCUSSION OF RESULTS

6.1 Containment Response and Pressure Capacity

Results of the nonlinear finite-element analysis confirmed that the most stressed section under design pressure, namely, the membrane hoop section near midheight of the cylinder remained the most stressed section all the way up to failure. This was true for both the prestressed and the reinforced concrete containments. This behavior was anticipated since: (i) the meridional flexural critical section at the containment wall-basemat junction is typically designed for discontinuity bending moments based on elastic analyses, which is conservative and (ii) unlike membrane tension, the discontinuity moment and shear do not increase linearly with internal pressure since the wall stiffness decreases more than linearly with pressure.

The structural response and pressure capacity obtained from the nonlinear finite element analysis and from equilibrium equations presented in Section 4 were virtually identical. The response of the prestressed concrete containment is shown in Figure 5.

The ultimate capacity of the containment is 228 psig which is about five times the design pressure of 45 psig and corresponds to incipient yielding of the hoop tendon in the membrane section near midheight of the cylinder. The response of the reinforced concrete containment is shown in Figure 6. The ultimate capacity of the containment is 95 psig which is 6.3 times the design pressure of 15 psig and corresponds to incipient yielding of the hoop rebars in the membrane section near midheight of the cylinder.

The ultimate capacities reported above are lower bound values for the concrete pressure boundary because of the conservative nature of the failure criteria defined in Section 3. Nonlinear analysis to realize the reserve capacity beyond the lower bound should be considered worthwhile only if the attendant large displacements can be functionally tolerated and if the pressure boundary not backed by concrete has matching or higher capacity.

A separate analysis was performed to determine the ultimate capacity of the pressure boundary not backed by concrete such as equipment hatch, personnel locks, electrical penetrations, steel drywell head, etc. Details of the analysis are outside the intended scope of this paper and therefore only the results are used for this discussion. The personnel airlock in the example prestressed concrete containment has a capacity of about 150 psig and the equipment hatch in the example reinforced concrete containment has a capacity of about 80 psig. This may be considered typical for containments where large steel penetration components are designed for 1.5 times the design pressure.

Based on the foregoing discussion, the authors feel that typically it will suffice to determine the ultimate pressure capacity of the concrete pressure boundary by using the equations presented in Section 4. Nonlinear finite element analysis or scaled model tests may be beneficial only where membrane sections of the concrete pressure boundary or steel pressure retaining components do not govern the ultimate pressure capacity.

6.2 Liner Leak-Tightness

The ASME Code, Section III, Division 2 on concrete containment design defines the allowable strains in the liner to ensure leak-tightness of the liner plate. With reference to these allowables, ultimate liner strains observed in the analyses did not indicate a potential for degradation of leak-tight integrity of the liner.

Liner strains in the reinforced concrete containment are shown in Figure 6. The maximum tensile strain in the liner at 95 psig, the ultimate capacity of the concrete pressure boundary, is 0.0024 in/in which is less than the code allowable value. At 80 psig, the ultimate capacity of steel pressure boundary, the liner strain is only 0.0021 in/in.

Liner strains in the prestressed concrete containment are shown in Figure 5. The liner strain at 228 psig, the ultimate capacity of the concrete pressure boundary, is 0.0054 in/in. At 150 psig, the ultimate capacity of the steel pressure boundary, the liner strain is below its yield limit. It should be noted that these strain levels exist only at the most stressed section and are lower at all other points. Therefore, greater overall leak-tightness is inferred.

The weld at liner seams has a substantially higher yield strength than the liner plate. Force equilibrium at liner seam will require that the stress at the seam

does not exceed the yield stress of the liner. Consequently, the strain level in the liner weld is not critical and is always less than its yield value.

The actual tensile strain level in the liner will be lower than the values discussed if imposed strains due to thermal expansion, creep, and shrinkage are also included.

6.3 Thermal Effects

Constraint to liner thermal expansion imposes compression in the liner and tension in the restraining containment wall. It is debatable if the liner would buckle under this compression when the high internal pressure tends to brace the liner against the concrete. Regardless, at ultimate pressure when general yielding of the reinforcing/prestressing steel occurs, restraint to the thermal expansion of the liner is fully relieved. Thus, thermal effects do not affect the computed ultimate capacity. This is true for creep and shrinkage effects also.

7. CONCLUSION

Based on the foregoing discussion, the following conclusions are in order:

a. The ultimate pressure capacity of concrete containments is several times their design pressure.

b. The hoop membrane section near midheight of the cylinder, which was the most stressed section under design pressure, remained the critical section all the way up to the ultimate pressure.

c. At membrane sections of the pressure boundary backed by concrete, the nonlinear response and ultimate capacity can be manually computed by means of the equilibrium equations and conservative failure criteria presented in this paper.

d. Nonlinear finite element analysis of the shell is recommended only if large displacements at true ultimate capacity can be tolerated and if a membrane section of the concrete pressure boundary or a steel pressure retaining component does not govern the ultimate capacity.

e. Computed liner strains indicate that the leak-tightness of the liner will not be impaired at the computed ultimate pressure.

f. Restrained deformation loads due to thermal expansion, creep, and shrinkage are relieved at ultimate pressure and do not affect the computed ultimate capacity.

REFERENCES

[1] GHOSH, S., WILSON, E.L, "Dynamic Stress Analysis of Axisymmetric Structures Under Arbitrary Loading," EERC Report 69-10, College of Engineering, University of California, Berkeley, April 1969.

[2] KHATUA, T.P., RADWAN, H.R., SARNE, Y., "Application of the Finite Element Method to the Nonlinear Analysis of RC Structures," ASCE Convention and Exposition, Chicago, October 16-20, 1978, Preprint 3427.

[3] LIN, C.S, SCORDELIS, A.C., "Nonlinear Analysis of RC Shells of General Form," Journal of the ASCE, Structural Division, Vol. 101, No. ST3, Proc. Paper 11164, March 1975, pp. 523-538.

[4] KAMIL, H., CHEN, M.C., KOST, G., MILLER, A., "Investigation of the Behavior of TMI-2 Containment Structure for Hydrogen Burn Accidents," Paper J5/8, SMiRT 6, Paris 1981.

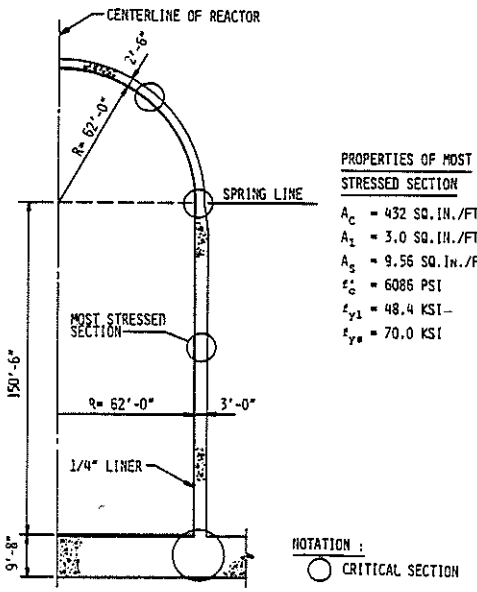

FIGURE 1. BWR MARK III REINFORCED CONCRETE CONTAINMENT

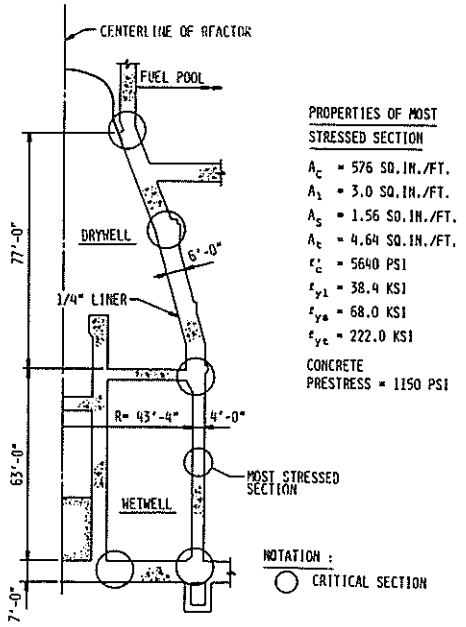

FIGURE 2. BWR MARK II PRESTRESSED CONCRETE CONTAINMENT

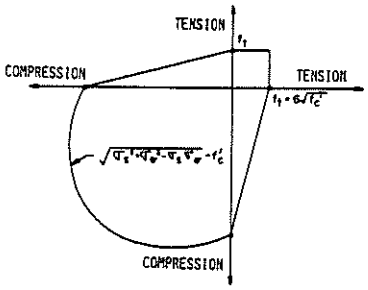

FIGURE 3. FAILURE CRITERION FOR CONCRETE UNDER BIAXIAL STRESS

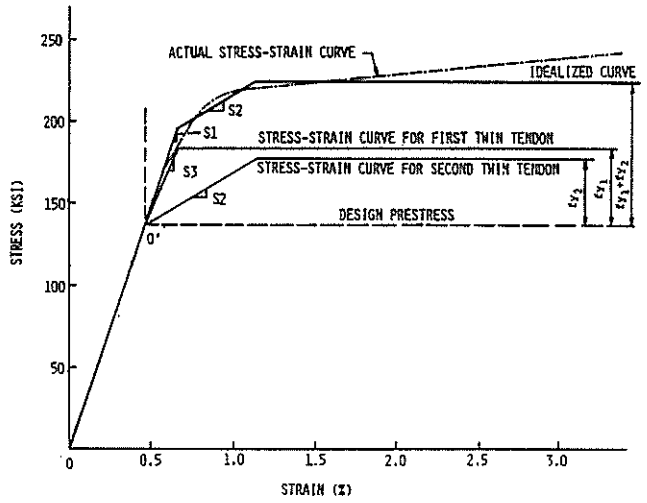

FIGURE 4. STRESS-STRAIN IDEALIZATION FOR POST-TENSIONING TENDONS

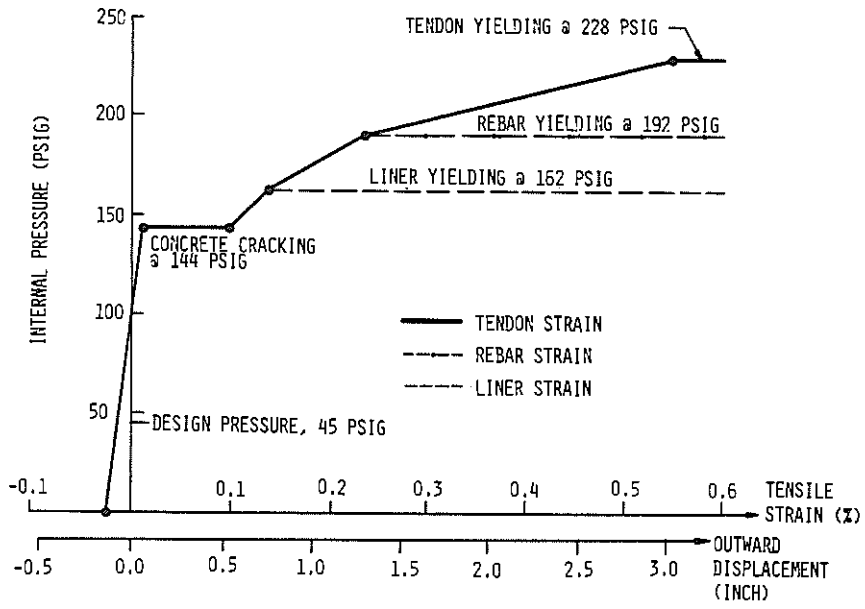

FIGURE 5. RESPONSE OF BWR MARK II PRESTRESSED CONCRETE CONTAINMENT AT THE MOST STRESSED SECTION

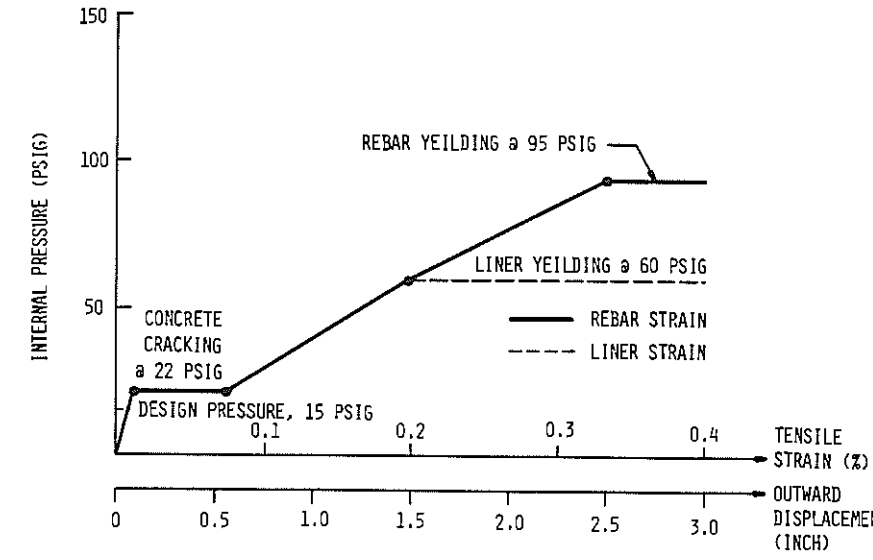

FIGURE 6. RESPONSE OF BWR MARK III REINFORCED CONCRETE CONTAINMENT AT THE MOST STRESSED SECTION